

## Bacterial control of silicon regeneration from diatom detritus: Significance of bacterial ectohydrolases and species identity

Kay D. Bidle<sup>1</sup> and Farooq Azam

Marine Biology Research Division, Scripps Institution of Oceanography, University of California San Diego-0202, 9500 Gilman Drive, La Jolla, California 92093

### Abstract

Bacteria (and possibly archaea) accelerate silica dissolution in the sea by colonizing and enzymatically degrading the organic matrix of diatom frustules. We tested whether colonizer species composition and ectohydrolase profiles critically control silicon regeneration by allowing diatom (*Thalassiosira weissflogii* and *Chaetoceros simplex*) detritus to be colonized by natural bacterial assemblages and 12 phylogenetically characterized marine isolates. We characterized the colonizers' ectohydrolase profiles and rates of silicon regeneration. The colonizers' cell-specific protease activity was consistently the dominant ectohydrolase, and it strongly correlated with silica dissolution rates. Cell-specific glucosidase, lipase, and chitinase activities showed no correlation with silicon regeneration. Denaturing gradient gel electrophoresis (DGGE) of PCR-amplified 16S rRNA genes was used to monitor colonization of detritus by natural microbial assemblages and to identify colonizing phylotypes. Representatives from gammaproteobacteria and sphingobacteria-flavobacteria classes dominated colonizer populations by comprising 65% and 25% of detected phylotypes, respectively. Archaea were not detected among colonizer populations. All bacterial isolates accelerated silica dissolution, but individual rates varied by >300%. Significant variability was observed within the *Alteromonadaceae*, which indicates different abilities to process diatom organic matter. Isolates that displayed enhanced colonization and protease activities were the most effective at regenerating silicon. The most effective isolate belonged to the sphingobacteria-flavobacteria, a group specialized in colonizing marine particles. Other effective isolates grouped with *Pseudoalteromonas*, *Alteromonas*, and *Vibrio* genera. One isolate caused intense aggregation of diatom detritus, significantly reducing silicon regeneration. Our results indicate that bacterial species identity strongly controlled silicon regeneration by influencing the colonization potential and ectohydrolytic profiles of bacteria as well as aggregate formation. Mechanistic models of oceanic silica cycling should incorporate species composition and ectohydrolase profiles of bacteria involved in silicon regeneration.

Diatoms often dominate phytoplankton communities in many oceanic systems, contributing significantly to total primary production as well as to downward fluxes of biogenic silica and organic matter (Sieracki et al. 1993; Honjo et al. 1995; Smith et al. 1996; Brzezinski et al. 1998). Since diatoms have an absolute silicon requirement for growth (Lewin 1962), the supply of silicic acid to diatoms in the euphotic zone critically controls diatom productivity. In fact, the availability of dissolved silicic acid has been shown to control diatom silica production rates, at least at times, in every natural system examined to date (Nelson and Brzezinski 1990; Nelson and Tréguer 1992; Brzezinski and Nelson 1996; Nelson and Dortch 1996; Brzezinski et al. 1998). Furthermore, Si control of production has recently been proposed for the equatorial Pacific upwelling system; numerical modeling indicated that the supply rate of silicic acid, rather than iron or nitrate, sets the upper limit on diatom production as well as export production (Dugdale et al. 1995; Dugdale and Wilkerson 1998). Empirical evidence from a number of oceanic systems has revealed that Si regeneration in the upper mixed layer, via dissolution of biogenic silica, is a crit-

ical Si supply mechanism to diatoms (Brzezinski and Nelson 1989, 1995; Nelson et al. 1995, 1996). These regions, where diatom silica is recycled more rapidly, possess a regenerated source of the required Si in addition to the exchange with new, nutrient-rich subsurface water. It has been estimated that an atom of Si is cycled 39 times before burial to the seabed (Tréguer et al. 1995), which illustrates that silicon regeneration is robust and efficient. Moreover, the extent of Si regeneration within the upper water column is quite substantial and sustains significant diatom production. This is expressed as a dissolution:production ( $D:P$ ) ratio, or the fraction of biogenic silica production supported by regenerated Si. The global average  $D:P$  ratio is 0.6 in the upper 200 m (Nelson et al. 1995). It exceeded 0.7 in some systems like a coastal upwelling area (Nelson and Goering 1977), a warm core ring (Brzezinski and Nelson 1989), and Ross Sea continental shelf waters (Nelson et al. 1996). Si dissolution can also profoundly affect nutrient dynamics within a system. Even modest Si regeneration (e.g.,  $D:P = 0.1$ ) can shift diatom production to N limitation, as documented for the Monterey Bay upwelling system (Brzezinski et al. 1997b); similar reasoning might apply to high-nutrient low-chlorophyll (HNLC) regions (e.g., equatorial Pacific and the Ross Sea), which may oscillate between Si and Fe limitation.

Even though regeneration is now known to play a major role in oceanic Si cycling, the mechanisms that regulate the process are not well understood. This is an important issue since Si regeneration is highly variable among oceanic systems ( $D:P$  ratios range from 0.05 to 5.8; Nelson et al. 1995).

### Acknowledgements

We thank Mark Brzezinski, Richard Long, and Kelly Bidle for helpful suggestions. This manuscript benefited from the comments of two anonymous reviewers. This research was supported by NSF grant OCE-9819603 to F.A.

<sup>1</sup> Present address: Institute of Marine and Coastal Sciences, Rutgers University, 71 Dudley Road, New Brunswick, New Jersey 08901-8521 (bidle@imcs.rutgers.edu).

Current biogeochemical models consider Si regeneration to be controlled by regional factors like surface temperature, selective zooplankton grazing, and aggregate formation (Nelson et al. 1995; Dugdale and Wilkerson 1998). Recently, we discovered a major role for bacteria (and possibly archaea) in the regeneration of diatom silica, providing mechanistic insight into the control of Si regeneration and diatom productivity in oceanic systems (Bidle and Azam 1999). Similar findings have been shown for lakes (Patrick and Holding 1985). Bacteria-mediated Si dissolution can account for the observed, efficient regeneration of diatom Si in the upper mixed layer as well as explain its variability. Thus, high and variable *D:P* ratios (0.5–0.8) for open ocean systems (Brzezinski and Nelson 1995; Nelson et al. 1995) can be interpreted as being caused mainly by bacteria, an idea strengthened by the findings that abiotic or protozoa-mediated dissolution is negligible (Bidle and Azam 1999) and that metazoa do not cause dissolution (Tande and Slagstad 1985).

Bacterial mediation of potentially rapid and highly variable silica regeneration rates must be regulated by multifaceted in situ controls on bacterial action on diatom frustules. For example, colonization intensity, rather than bulk phase bacterial abundance, appeared to control silicon regeneration since it was accompanied by very strong and rapid colonization of diatom detritus by bacteria (Bidle and Azam 1999). Therefore, insights into critical control mechanisms must be sought in the colonizing population. Does colonization alone lead to regeneration of diatom Si, or are there other controls as well? Colonizing bacteria expressed extremely high levels of ectoprotease activity (compared to bulk phase), efficiently hydrolyzing the organic matrix protecting diatoms from dissolution. However, it is not known whether an array of ectohydrolytic enzymes are required for enhanced Si regeneration, since the aforementioned study only documented protease activity. Bacteria are known to possess a suite of other ectohydrolytic enzymes (e.g., glucosidase, lipase, and chitinase) capable of hydrolyzing different classes of macromolecules. The expression of specific hydrolytic enzymes by colonizing bacteria may determine whether silicon regeneration is slow or rapid in nature. Moreover, species identity of bacterial colonizers likely controls Si regeneration by influencing colonization patterns and the effectiveness of ectoenzymes that hydrolyze the protective organic matrix. Also, certain bacterial phylotypes may possess the ability to preferentially respond to diatoms and cause extensive silica cycling.

The goal of this study is to explore the critical controls on bacteria-mediated Si regeneration by identifying the sources of variability seen in dissolution of particulate diatom silica. Specifically, we examine the importance of colonizer species identities and their attendant ectohydrolytic enzyme profiles. Our broad goal is to contribute to the mechanistic understanding of silicon biogeochemistry and to predictive models of silica dynamics within oceanic systems.

## Materials and methods

*Growth and maintenance of diatoms and bacteria*—Axe-  
nic cultures of *Thalassiosira weissflogii* and *Chaetoceros*

*simplex* were obtained from the Provasoli-Guillard Center for Culture of Marine Phytoplankton (West Boothbay Harbor, Maine). Batch cultures were grown in f/2 liquid medium (Guillard 1975) by rotary shaking (70 rpm) under 14:10 light:dark cycle. Illumination was with cool white light at  $\sim 200 \mu\text{E s}^{-1} \text{ cm}^{-2}$ . Late-exponential phase cultures were harvested; washed once with 0.22- $\mu\text{m}$  filtered, autoclaved seawater (FASW); and resuspended in FASW. Cell suspensions were made into fresh diatom detritus by rapidly freeze (dry-ice/ethanol bath) thawing (55°C water bath) for seven cycles. Lack of cellular ATP or growth in f/2 medium confirmed in a previous test of the procedure that cells were dead. Detritus was stored at  $<20^\circ\text{C}$  until further use. Acid-treatment of diatom detritus, where necessary, was performed as in Lewin (1961).

Marine bacteria were isolated on ZoBell 2216E agar (5 g peptone, 1 g yeast extract and 15 g bacto agar per liter of 0.7- $\mu\text{m}$  filtered seawater). Most bacteria (Tw1 to Tw10) were isolated from incubations of natural bacterial assemblages with *T. weissflogii* detritus, whereas others were isolated during “bottle bloom” experiments on 23 September 1993. Isolates were grown in batch preparations of ZoBell 2216E broth while shaking (125 rpm) at 15°C.

*Experimental setup*—Silicon regeneration experiments used diatom detritus suspended in seawater containing natural bacterial assemblages, bacterial isolates, or FASW. Incubations also used acid-treated diatom frustules resuspended in FASW. FASW represented an abiotic medium.

Natural bacterial assemblages were obtained by filtering seawater samples from Scripps Pier through Whatman filters (GF/F, 0.7- $\mu\text{m}$  pore size) under low pressure differential ( $<12 \text{ cm Hg}$ ). Filtration removed unknown particulate organic matter before adding detritus. Microscopy confirmed that this procedure also removed heterotrophic flagellates.

For experiments using bacterial isolates, bacteria were grown in ZoBell 2216E medium until mid- to late-exponential phase, to minimize the presence of dead cells. Cultures were harvested (3,000 g, 10 min, 10°C), washed free of growth medium with FASW, and resuspended in FASW (final bacterial cell concentration  $\sim 10^6 \text{ ml}^{-1}$ ). Cells remained suspended in FASW for 4 h at 15°C prior to addition of detritus.

Diatom detritus was added to achieve 800  $\mu\text{g C L}^{-1}$  POC. These additions corresponded to  $10^4$  and  $10^5$  cells  $\text{ml}^{-1}$  for *T. weissflogii* and *C. simplex*, respectively. For acid-treated incubations, equal cell concentrations were used. Incubations were in 300–1,000-ml Nalgene bottles with rotary shaking at 18°C.

*Silicon regeneration measurements*—Silicic acid was measured spectrophotometrically by the silicomolybdate method (Parsons et al. 1984). Aliquots were removed from incubation vessels, particulate material was pelleted (3,000  $\times$  g, 15 min, 10°C), and the supernatant assayed for silicic acid. Total silica budgets were determined by a hot sodium hydroxide hydrolysis technique (Werner 1966). All incubations and assays were done in sterile polypropylene containers. Si regeneration was determined both as the percentage particulate silica dissolved and as the specific dissolution rate

( $V_{\text{dis}}$ ;  $\text{d}^{-1}$ ). Calculations for  $V_{\text{dis}}$  are based on Hurd and Birdwhistell (1983).

**Ectohydrolytic activities**—Activities for total and  $<3.0\text{-}\mu\text{m}$  filtered fractions were measured during the course of experiments. Cell-specific rates for attached bacteria were obtained on the basis of the difference between total and  $<3.0\text{-}\mu\text{m}$  fractions. Ectohydrolytic activities were measured using commercially available substrates using either amino-4-methylcoumarine (AMC) or methylumbelliferone (MUF) as the fluorophore (Hoppe 1983). Numerous substrates were used to assay protease and glucosidase activities (protease = Leuine-AMC, Glycine-AMC, Serine-AMC, and Threonine-AMC; glucosidase = MUF- $\alpha$ -D-glucoside, MUF- $\beta$ -D-glucoside, MUF-xyloside, and MUF-mannopyranoside), whereas MUF-oleate and MUF-N-acetyl- $\beta$ -D-glucose-amine were used to assay lipase and chitinase, respectively. Substrates were added at  $100\text{-}\mu\text{M}$  final concentration. Hydrolysis was monitored by measuring fluorescence during timed incubations. Samples were incubated at the in situ temperature ( $18^{\circ}\text{C}$ ) in the dark. Assays were usually done in triplicate; one sample was boiled ( $100^{\circ}\text{C}$ ) before adding substrate and served as control. Fluorescence was measured in cuvettes or flat-bottomed, white microtiter plates (Falcon) using a Hoefer TKO-100 fluorometer (Excitation =  $365\text{ nm}$ ; Emission =  $460\text{ nm}$ ) or a HTS 7000 Series BioAssay microtiter plate fluorometer (Excitation =  $360\text{ nm}$ ; Emission =  $465\text{ nm}$ ; Perkin Elmer), respectively. Each instrument was calibrated with 7-amino-4-methylcoumarine and methylumbelliferone.

**Microscopy**—Bacteria were counted by epifluorescence microscopy. Aliquots were fixed in 2% formalin. Unless stained immediately, samples were stored at  $4^{\circ}\text{C}$  until processing. Total fractions were treated with  $10\text{-}\mu\text{g ml}^{-1}$  Tween 80 (final concentration) and sonicated for 1 min at full power using a sonic dismembrator 50 (Fisher Scientific) prior to staining. A sonication step was not used for  $<3.0\text{-}\mu\text{m}$  filtrates. All samples were stained with 4-6-diamidino-2-phenylindole (DAPI) at a final concentration of  $1\text{-}\mu\text{g ml}^{-1}$  for 10 min. Samples were filtered onto  $0.2\text{-}\mu\text{m}$ , black Poretics polycarbonate track-etched (PCTE) membrane filters. Slides were examined at  $1000\times$  magnification (Olympus BH-2).

Bacterial colonization of diatoms was quantified as follows: 7–10 ml of DAPI-stained, total water samples (unsonicated sample) were gravity filtered onto  $3.0\text{-}\mu\text{m}$ , Poretics PCTE membrane filters prestained with Irgalan black (2% w/v in 2% acetic acid). All filters were rinsed with an equal volume of FASW to remove unattached or loosely associated bacteria. Average colonization intensities were obtained by counting the number of attached bacteria on at least 30 individual diatom cells.

**DNA extraction from communities and bacterial isolates**—Diatoms and their associated microbes were collected by gravity filtration of total sample ( $\sim 300\text{ ml}$ ) onto  $47\text{-mm}$   $3\text{-}\mu\text{m}$  pore-size PCTE membrane filters. Filters were stored in a sterile centrifuge tube at  $-20^{\circ}\text{C}$  until processed. DNA was extracted according to Fuhrman et al. (1988) with volume modification. Each frozen filter was thawed, vortexed

briefly in 2 ml STE (sodium chloride-Tris-EDTA) buffer (10 mM Tris-HCl [pH 8], 1 mM  $\text{Na}_2\text{EDTA}$  (ethylenediamine-tetraacetic acid), 100 mM NaCl), and boiled for 2 min following addition of 0.1 volume of 10% sodium dodecyl sulfate (SDS). Extracts were poured into a clean, sterile 15 ml centrifuge tube (Corex), and the filter was rinsed with 1 ml of STE buffer. Rinsate and lysate volumes were pooled. Remaining extraction procedures followed described protocol (Fuhrman et al. 1988). Extracted DNA was resuspended in  $200\text{-}\mu\text{l}$  TE buffer (10 mM Tris-HCl, 1 mM  $\text{Na}_2\text{EDTA}$  [pH 8]) and quantified fluorimetrically using Picogreen (Molecular Probes).

For bacterial isolates, DNA was isolated from approximately  $10^9$  cells in late-exponential phase using the DNeasy tissue kit (Qiagen) according to manufacturer's instructions and was suspended in TE buffer.

**PCR amplification**—Bacterial and archaeal 16S rRNA genes were amplified from community DNA using polymerase chain reaction (PCR). For bacteria, a universal 17-mer primer complementary to position 517–534 (5'-AT-TACCGCGCTGCTGG-3'; 534R) and a bacterial primer complementary to position 341–358 plus a GC clamp (5'-CGCCCCCGCGCGCGCGGGCGGGGCGGGGGC-ACGGGGGGG-CCTACGGGAGGCAGCAG-3'; GC341F) were used. The 40 bp GC clamp (underlined) was attached to the bacterial primer to prevent complete melting of amplicons during denaturing gradient gel electrophoresis (DGGE; Sheffield et al. 1989; Muyzer et al. 1993). For archaea, Arch21F (TTCCGGTTGATCCYGCCGGA-3') and Arch958R (5'-YCCGGCGTTGAMTCCAATT-3') were used (DeLong 1992). PCR reactions ( $50\text{-}\mu\text{l}$ ) contained 20 mM Tris-HCl (pH 8.4), 50 mM KCl, 2.5 mM  $\text{MgCl}_2$ , 0.8 mM deoxynucleotide triphosphates,  $0.5\text{-}\mu\text{M}$  of each primer, 2.5 units of Taq DNA polymerase (Gibco BRL, Life Technologies), and 50–100 ng of template DNA. Initial denaturation was at  $94^{\circ}\text{C}$  for 5 min followed by a thermal cycling program: denaturation for 1 min at  $94^{\circ}\text{C}$ ; primer annealing for 1 min at an initial  $65^{\circ}\text{C}$ , decreasing  $1^{\circ}\text{C}$  every two cycles to a final annealing temperature of  $50^{\circ}\text{C}$  ("Touchdown" PCR; Don et al. 1991); primer extension for 3 min at  $72^{\circ}\text{C}$ . Thirty cycles were run followed by 7 min of final extension at  $72^{\circ}\text{C}$ . Negative controls where template volumes were replaced by sterile water (MilliQ-purified and autoclaved) were run in each batch of PCR reactions. PCR products were verified by agarose gel electrophoresis.

The 16S rRNA genes of bacterial isolates were amplified using 50–100 ng of genomic DNA in PCR reactions using the following bacterial-specific primers: 27F (5'-AGAGTTTGATCM TGGCTCAG-3') and 1492R (5'-TACGGYTACCTTGTACGACTT-3'). Initial denaturation was at  $94^{\circ}\text{C}$  for 5 min followed by a thermal cycling program: denaturation for 1 min at  $94^{\circ}\text{C}$ ; primer annealing for 1 min at  $55^{\circ}\text{C}$ ; primer extension for 2 min at  $72^{\circ}\text{C}$ . Thirty cycles were run followed by 5 min of final extension at  $72^{\circ}\text{C}$ . PCR products were verified by agarose gel electrophoresis.

**DGGE**—PCR products from triplicate reactions were pooled and cleaned using the ultra-clean PCR clean-up Kit (Mo Bio Laboratories) according to manufacturer's instruc-

Table 1. Effect of bacterial protease inhibition on particulate silica dissolution from diatom detritus.

Diatom	Condition	Cell-specific protease activity* (amol cell <sup>-1</sup> h <sup>-1</sup> )	Particulate Si dissolved† (%)
<i>T. weissflogii</i>	untreated control‡	438–2032	15 ± 1.5
	protease inhibitor§	nd	1.9 ± 0.7
<i>C. simplex</i>	untreated control	214–725	42 ± 5.6
	protease inhibitor	nd	4.9 ± 7.0

\* Range of average leucine-AMC hydrolysis through 7 d.

† After 10 d.

‡ Diatom detritus added to GF/F filtered seawater.

§ 170 µg ml<sup>-1</sup> phenylmethylsulfonyl fluoride and 0.5 µg ml<sup>-1</sup> leupeptin added to untreated control.

nd = none detected.

tions. Products were suspended in TE buffer and quantified using Picogreen, and 600–1,000 ng was loaded on 8% polyacrylamide gels (acrylamide : N,N'-methylbisacrylamide 37 : 1) containing denaturant gradients of 30–50% top to bottom (100% denaturant is defined as 7 M urea and 40% [vol/vol] formamide). Electrophoresis was run at 200 V for 6 h in a hot bath DGGE unit (CBS Scientific) using 0.5× TAE (20 mM Tris, 10 mM acetic acid, 0.5 mM Na<sub>2</sub>EDTA, pH 8.2) as running buffer. Gels were stained with 1× SYBR Green (1 : 10,000 dilution of stock) for 30 min followed by a 10 min destain in 0.5× TAE. Bands were visualized using a Nucleovision gel capturing system equipped with UV transillumination, a CCD camera, and image analysis software (Nucleotech).

Bands were excised using a sterile scalpel blade, and the DNA was eluted overnight at 37°C in 400 µl 1× SSC buffer (0.6 M NaCl, 60 mM sodium citrate, pH 7). Eluents were transferred to a fresh 1.8-ml Eppendorf tube and the acryl-

amide fragment was washed once with 100-µl SSC. Volumes were pooled and precipitated with 0.8 M LiCl<sub>2</sub> and 70% ethanol overnight at -20°C (Sambrook et al. 1989). Precipitated DNA was pelleted by centrifugation (23,000 × g; 15 min; 4°C), washed once with 70% ethanol, and dried at room temperature. DNA was resuspended in 10 µl TE. Bands were reamplified in order to increase the amount of material for cloning. Amplicons were cloned using the TOPO TA cloning kit (Invitrogen), and the presence of inserts was verified by digestion of plasmid DNA with EcoRI or by PCR screening according to manufacturer's instructions. DGGE profiles of reamplified, cloned DNA were used to check for heteroduplexes and to confirm the position of cloned bands relative to the original sample (Riemann et al. 1999).

**Sequencing and phylogenetic analysis**—Bidirectional sequencing was performed with the ABI PRISM sequencing kit (Perkin Elmer) using an automated ABI DNA sequencer. Sequences were aligned to known sequences using BLAST (basic local alignment search tool; Altschul et al. 1990). Phylogenetic relationships were inferred by neighbor joining method using Clustal W (Thompson et al. 1994). Clustal W uses sequence weighting, position-gap penalties, and weight matrix choice to improve the sensitivity of progressive multiple sequence alignments. Taxonomic relationships and identities are based on <http://www.cme.msu.edu/bergeys/april2001-genus.pdf>. Sequences obtained in this study can be obtained at <http://www.ncbi.nlm.nih.gov/>. Accession numbers for bacterial isolates are AY028196–AY028207.

## Results

**Si regeneration**—Profiles of particulate silica dissolution from *T. weissflogii* and *C. simplex* detritus incubating under various conditions are shown in Fig. 1. Little to no disso-

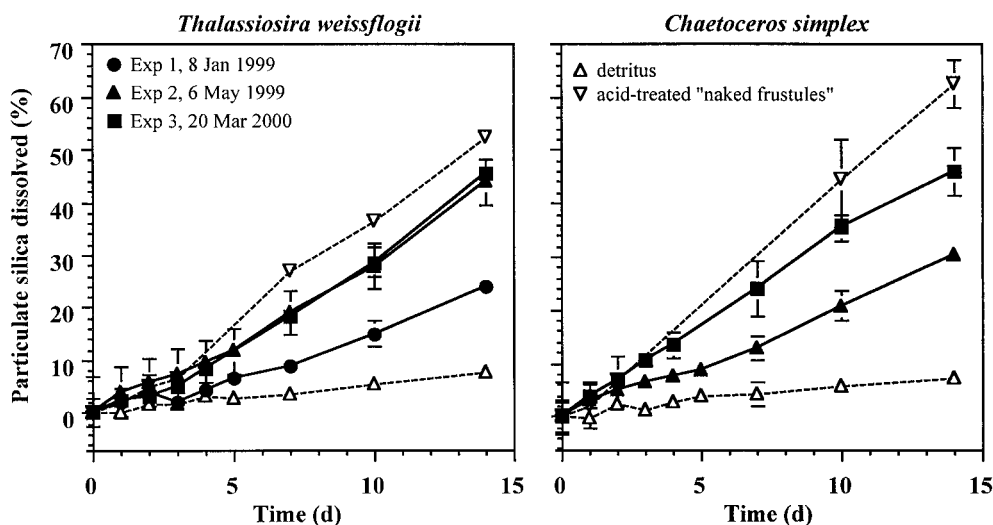


Fig. 1. Time course of particulate silicon regeneration from diatom detritus incubating under different conditions. Diatom detritus was added to natural, bacterial assemblages collected off of Scripps Pier on 3 different days (solid symbols). Open symbols represent control incubations where diatoms were resuspended in abiotic seawater.

lution was observed for experiments containing intact diatom detritus incubating in abiotic seawater. Specific dissolution rates ( $V_{\text{dis}}$ ) for these samples were consistently low (0.004–0.009  $\text{d}^{-1}$ ) for both diatoms. Results for one experiment are shown since the rates for different experiments were similar. In contrast, bacteria-mediated Si regeneration was generally rapid for samples containing either *T. weissflogii* or *C. simplex*. Incubations containing natural bacterial assemblages consistently enhanced the dissolution of diatom silica, but there was considerable variation for samples containing different source populations of bacteria. For *T. weissflogii*,  $V_{\text{dis}}$  was twice as high for experiments 2 and 3 (0.035  $\text{d}^{-1}$  and 0.032  $\text{d}^{-1}$ , respectively) than for experiment 1 (0.016  $\text{d}^{-1}$ ). Rates were the same for experiments 2 and 3 even though natural bacterial assemblages were collected nearly 1 yr apart. Variability was also seen for incubations containing *C. simplex* where Si regeneration rates differed by two-fold between experiments 2 (0.026  $\text{d}^{-1}$ ) and 3 (0.051  $\text{d}^{-1}$ ). The natural bacterial assemblage collected for experiment 1 was not used with *C. simplex*. Bacteria-mediated Si regeneration was similar but not quite as rapid as that of acid-cleaned frustules incubating in abiotic seawater. These samples contained axenic detritus from which the organic matrix had been hydrolyzed prior to incubation. Specific dissolution rates were 0.051  $\text{d}^{-1}$  and 0.073  $\text{d}^{-1}$  for *T. weissflogii* and *C. simplex*, respectively.

**Colonizer enzyme profile**—Cell-specific ectoprotease activities ( $\text{amol cell}^{-1} \text{h}^{-1}$ ) of colonizing bacteria were consistently the highest activity measured on diatom detritus (Fig. 2; note scale) and were generally comparable between the two diatoms. Of the substrates used to measure protease activity, Leuine-AMC consistently yielded the highest hydrolysis rates throughout the 7 d sampling period with activity generally peaking after 2–3 d (Fig. 2A). Cell-specific hydrolysis rates of colonizing bacteria were also elevated for Glycine-AMC and Serine-AMC; during the first 2 d they exceeded Leuine-AMC hydrolysis. Of the four substrates used to measure protease activity, Threonine-AMC consistently yielded the lowest cell-specific hydrolysis rates with values <250  $\text{amol cell}^{-1} \text{h}^{-1}$ .

Cell-specific glucosidase rates were much lower than protease rates, regardless of substrate (Fig. 2B). Hydrolysis rates for bacteria colonizing *T. weissflogii* detritus generally ranged from <1 to ~20  $\text{amol cell}^{-1} \text{h}^{-1}$  for each experiment (except for experiment 2 where  $\alpha$ -glucosidase activity reached approximately 50  $\text{amol cell}^{-1} \text{h}^{-1}$  on day 1). Cell-specific hydrolysis rates for bacteria colonizing *C. simplex* detritus were similar to those observed for *T. weissflogii* detritus except for higher initial rates (day 1) during experiment 2 for most substrates.

Cell-specific lipase rates of bacterial colonizers were moderate and fell between protease and glucosidase activities (Fig. 2C). Lipase activities showed considerable variability between the two diatoms. Experiment 3 had elevated activities in incubations with *T. weissflogii* detritus, whereas experiment 2 had elevated activities in incubations with *C. simplex* detritus.

**Relationship between silica dissolution and enzyme profiles**—Experiments showing enhanced Si regeneration were characterized by elevated protease activity. For *T. weissflogii*, daily cell-specific hydrolysis rates of Leuine-AMC, Glycine-AMC, and Serine-AMC were as much as 20-, 15-, and 40-fold higher, respectively, during experiments 2 and 3 than during experiment 1. Statistical analysis (paired *t*-test) comparing average Leuine-AMC hydrolysis over the course of experiments revealed highly significant differences between experiments 1 and 2 ( $p = 0.004$ ) and between experiments 1 and 3 ( $p = 0.0013$ ). Significant differences ( $p < 0.05$ ) were also observed for Glycine-AMC and Serine-AMC hydrolysis. The same analysis found no significant difference between experiments 2 and 3 ( $p = 0.8469$ ), which indicates similar levels of protease activity on diatom detritus. Elevated cell-specific protease activity of bacterial colonizers also correlated well with enhanced Si regeneration from *C. simplex*. This was especially evident in the first few days of experiment 3. Daily cell-specific hydrolysis rates for Leuine-AMC and Serine-AMC were on average twice those in experiment 2, whereas Glycine-AMC hydrolysis rates were nearly eight times higher in experiment 3 on day 1. Also, the natural bacterial assemblage to which diatoms were added for incubation in experiment 3 had 20- to >100-fold higher cell-specific protease activity than experiment 2 (depending on substrate used).

Glucosidase and lipase activities of bacterial colonizers had no consistent relationship with Si regeneration from diatom detritus. For *T. weissflogii*, the ratio of daily cell-specific glucosidase activities of experiments 2 and 3 to that of experiment 1 was often <1, which indicates that experiments 2 and 3 had lower glucosidase activities than experiment 1. A paired *t*-test comparing average cell-specific  $\beta$ -glucosidase activities between all three experiments revealed no significant differences ( $p = 0.1233$ – $0.4982$ ). Differences in cell-specific lipase activities were not observed for experiments 1 and 2, yet these two experiments had very different Si regeneration rates. Additionally, experiment 3 showed elevated cell-specific lipase activities during days 2–4 but Si regeneration was identical to experiment 2. For *C. simplex*, elevated glucosidase and lipase activities of bacterial colonizers during experiment 2 did not translate into more efficient Si regeneration.

**Inhibition of protease activity**—The addition of protease inhibitors (170  $\mu\text{g ml}^{-1}$  phenylmethylsulfonyl fluoride and 0.5  $\mu\text{g ml}^{-1}$  leupeptin) to incubations exposing diatom detritus to natural bacterial assemblages completely abolished bacterial protease activity (Table 1). Samples showed little to no silica dissolution after 10 d and resembled abiotic controls. Incubations devoid of protease inhibitors had high bacterial protease activities and led to an order of magnitude increase in particulate silica dissolution after 10 d.

**Composition of colonizers**—Amplification of 16S rRNA from colonizer community DNA was only successful using bacterial primers; amplification was not achieved using primers specific for archaea. DGGE profiles of bacterial communities colonizing diatom detritus during experiments 2 and 3 are shown in Fig. 3. The profiles provided a finger-



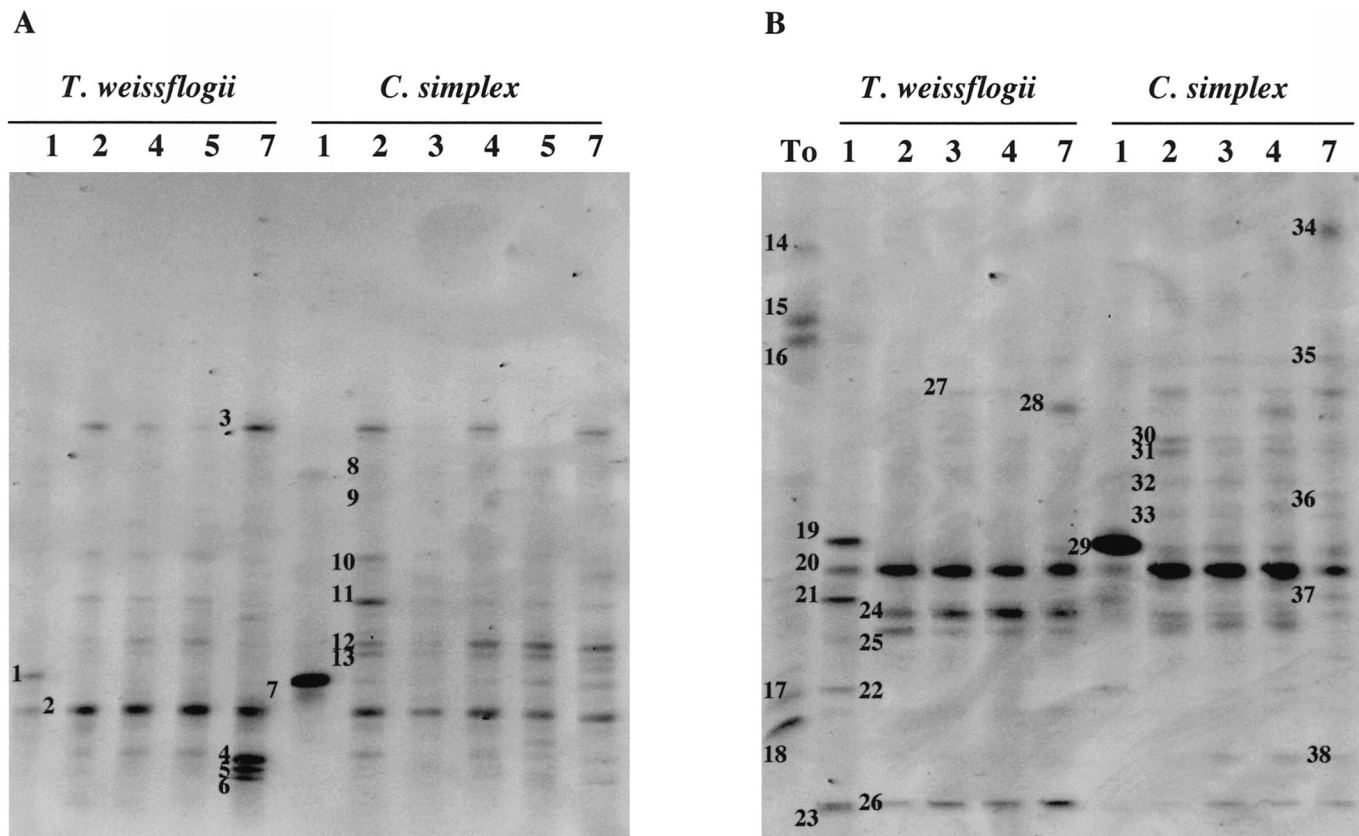


Fig. 3. DGGE profiles characterizing the community composition of bacteria colonizing diatom detritus during microcosm incubations. Results are shown for two separate experiments using natural marine bacterial assemblages collected at different times: (A) exp 2, 6 May 1999; (B) exp 3, 20 March 2000. A denaturing gradient of 30–50% was used for each gel. Numbers above each lane indicate the time (in days) after which diatoms were added to bacterial assemblages (GF/F-filtered seawater). “T<sub>0</sub>” in (B) refers to the bacterial assemblage prior to addition of diatom detritus. Each excised, cloned, and sequenced band is numbered. The relationships of excised band sequences to other sequences in the GenBank database are listed in Table 2.

print of bacterial colonization dynamics over the course of each experiment. Fingerprints revealed bacterial species richness (i.e., number of bands) associated with diatom detritus during incubation with natural bacterial assemblages collected at different times.

Experiment 2 was characterized by one to two phylotypes at 1 d (Fig. 3A; bands 1, 2, 7) followed by a burst of 6–10 phylotypes after 2 d. In general, the phylotypes detected at 2 d persisted throughout the measurement period (7 d), which indicates vigorous colonization. A second burst of diversity was detected for *T. weissflogii* at 7 d with the addition of three more dominant phylotypes (bands 4, 5, 6). Experiment 3 was characterized by a much stronger initial diversity of bacterial colonizers on both diatoms at 1 d. *T. weissflogii* was initially colonized by five phylotypes (bands 19–23) followed by a slight shift in the diversity profile at 2 d (disappearance of bands 19, 21, 22, and 23 and the appearance of bands 24–26). Similarly, *C. simplex* was initially colonized by five phylotypes (bands 20–22, 29, 32) followed by a strong burst of diversity at 2 d (addition of bands 24–25, 27, 30–33). In general, the phylotypes detected at 2 d persisted throughout the sampling period.

The sequencing of excised bands allowed us to identify their relationships to other known sequences in the GenBank

database. Figure 4 shows the phylogenetic relationships of excised band sequences to each other and to representative sequences in the GenBank database. Table 2 lists the closest relative to each excised band. Some band sequences had identical blast bit scores and percentage identities to multiple sequences in GenBank. In these cases, a representative is listed as the closest relative. Phylogenetic analysis revealed the dominance of two major classes of bacteria, the  $\gamma$ -proteobacteria and the sphingobacteria-flavobacteria (SFB). Sixty-five percent (21 of 33) of the colonizing phylotypes belonged the  $\gamma$ -proteobacteria and most of these were within the *Alteromonadaceae* family (Fig. 4A). Phylotypes most closely related to *Pseudoalteromonas atlantica* (COL-2, COL-4), *Pseudoalteromonas* sp. A3 (COL-25), and an unclassified *Pseudomonas* (COL-24) were the most rigorous colonizers of both *T. weissflogii* and *C. simplex* detritus in both experiments (Table 2). These phylotypes consistently colonized the diatoms at 1 d and persisted as the dominant colonizer throughout the experiment. Full-length sequences (194 bp) of bands 2 and 20 were found to be identical. Other phylotypes within the  $\gamma$ -proteobacteria preferentially colonized *C. simplex* detritus (COL-13, COL-30 to 33, COL-36, COL-38) accounting for a higher diversity of bacterial phylotypes on *C. simplex*, especially in experiment 3 (Fig. 3B).

Table 2. Relationship of excised band sequences to other sequences in the GenBank database.

Band	Clone ID	Accession number*	Closest relative†	Percent-identity‡	Phylogenetic grouping
<i>Experiment 2</i>					
1	PL-1	AY028208	Uncultured marine eubacterium MEB6	98	Plastid
2	COL-2	AY028401	<i>Pseudoalteromonas atlantica</i> ‡	100	$\gamma$ -proteobacteria, alteromonadales
3	COL-3	AY028402	Uncultured cytophagales clone CRE-PA37	100	Sphingobacteria/flavobacteria
4	COL-4	AY028172	<i>Pseudoalteromonas atlantica</i> ‡	96	$\gamma$ -proteobacteria, alteromonadales
5	COL-5	AY028173	<i>Shewanella violacea</i>	96	$\gamma$ -proteobacteria, aeromonadales
6	COL-6	AY028174	<i>Aeromonas jandaei</i> strain MTCC 3249‡	96	$\gamma$ -proteobacteria, aeromonadales
7	PL-2	AY028209	Unidentified eukaryotic clone OM20	98	Plastid
8	COL-8	AY028175	<i>Cytophaga</i> sp. strain JTB250	86	Sphingobacteria/flavobacteria
9	COL-9	AY028176	Saltmarsh clone LCP-72	96	Sphingobacteria/flavobacteria
10	COL-10	AY028177	Gamma proteobacterium HTB082	94	$\gamma$ -proteobacteria
11	COL-11	AY028178	Gamma proteobacterium HTB082	93	$\gamma$ -proteobacteria
12	Heteroduplex	—	—	—	—
13	COL-13	AY028179	<i>Colwellia demingiae</i> ACAM 606	96	$\gamma$ -proteobacteria
<i>Experiment 3</i>					
14	FL-14	AY028180	Unidentified cytophagales OM271	95	Sphingobacteria/flavobacteria
15	FL-15	AY028181	Unidentified beta proteobacterium OM43	98	$\beta$ -proteobacteria
16	FL-16	AY028182	Unidentified cytophagales OM271	97	Sphingobacteria/flavobacteria
17	FL-17	AY028183	Uncultured actinomycete OCS155	99	Actinobacteria
18	FL-18	AY028403	Uncultured Roseobacter NAC11-7	100	$\alpha$ -proteobacteria
19	PL-1	AY028208	Uncultured marine eubacterium MEB6	98	Plastid
20	COL-2	AY028401	<i>Pseudoalteromonas atlantica</i> ‡	100	$\gamma$ -proteobacteria, alteromonadales
21	COL-21	AY028404	Uncultured cytophaga ATT8	100	Sphingobacteria/flavobacteria
22	COL-22	AY028405	Unidentified bacterium oxSCC-14	100	$\gamma$ -proteobacteria; pseudomonadales
23	COL-23	AY028184	<i>Bradyrhizobium</i> sp. ORS285‡	99	$\alpha$ -proteobacteria, rhizobiales
24	COL-24	AY028185	Unclassified pseudomonas	95	$\gamma$ -proteobacteria; alteromonadales
25	COL-25	AY028186	<i>Pseudoalteromonas</i> sp. A3	96	$\gamma$ -proteobacteria; alteromonadales
26	COL-26	AY028187	<i>Ferrimonas balearica</i>	97	$\gamma$ -proteobacteria; aeromonadales
27	COL-27	AY028188	Unidentified bacterium isolate HOS19	99	Sphingobacteria/flavobacteria
28	COL-28	AY028189	Unidentified bacterium isolate HOS19	94	Sphingobacteria/flavobacteria
29	PL-2	AY028209	Unidentified eukaryotic clone OM20	98	Plastid
30	COL-30	AY028406	Gamma proteobacterium strain HTC042	100	$\gamma$ -proteobacteria; pseudomonadales
31	COL-31	AY028190	<i>Alteromonas</i> sp.	97	$\gamma$ -proteobacteria
32	COL-32	AY028191	Marine gamma proteobacterium MBE11	93	$\gamma$ -proteobacteria
33	COL-33	AY028192	Marine eubacterial sp. FL5	93	$\gamma$ -proteobacteria
34	Heteroduplex	—	—	—	—
35	COL-35	AY028193	Marine psychrophile SW17	97	Sphingobacteria/flavobacteria
36	COL-36	AY028407	<i>Vibrio</i> sp. Da4	100	$\gamma$ -proteobacteria, vibriales
37	COL-37	AY028194	<i>Vibrio</i> sp. SK1	99	$\gamma$ -proteobacteria, vibriales
38	COL-38	AY028195	<i>Aeromonas media</i> ‡	96	$\gamma$ -proteobacteria, aeromonadales

\* For sequences obtained in this study; nucleotide sequences can be accessed via <http://www.ncbi.nlm.nih.gov/>.

† Sequences were aligned to the closest relative using BLAST (Altschul et al. 1990). Identities were calculated excluding gaps.

‡ Clone sequence had multiple relatives with same percentage identity.

These phylotypes were most closely related to *Colwellia demingiae*, *Acinetobacter junii*, *Alteromonas* sp., an unidentified phylotype from marine macroaggregates (Eubacterial sp. FL5), *Vibrio* sp., and *Aeromonas* sp. (Table 2).

Bacterial phylotypes representing the SFB group constituted 21% (7 of 33) of the colonizing phylotypes. In general, SFB phylotypes detected in this study were most closely related to numerous uncultured *Cytophaga* detected on particles in various environments (Fig. 4B; Table 2). The dynamics of colonization for SFB phylotypes were not as consistent as those seen for the  $\gamma$ -proteobacteria representatives. Some SFB phylotypes colonized early in the experiment (by

2 d) and persisted throughout the experiment (COL-3, COL-8, and COL-9 in experiment 2 for both diatoms; COL-27 in experiment 3 for *C. simplex*). Other SFB phylotypes emerged on diatom detritus only later in the experiment (3–7 d) (COL-27, COL-28, COL-35 in experiment 3). One SFB phylotype in experiment 3 disappeared after colonizing both diatoms at 1 d (Fig. 3B; COL-21), which suggests rapid turnover for this particular colonizer. Several SFB phylotypes were not good colonizers of diatom detritus since they were detected in the free-living inoculum community but failed to develop on either diatom (FL-14, FL-16).

Representatives from both the  $\alpha$ - and  $\beta$ -proteobacteria

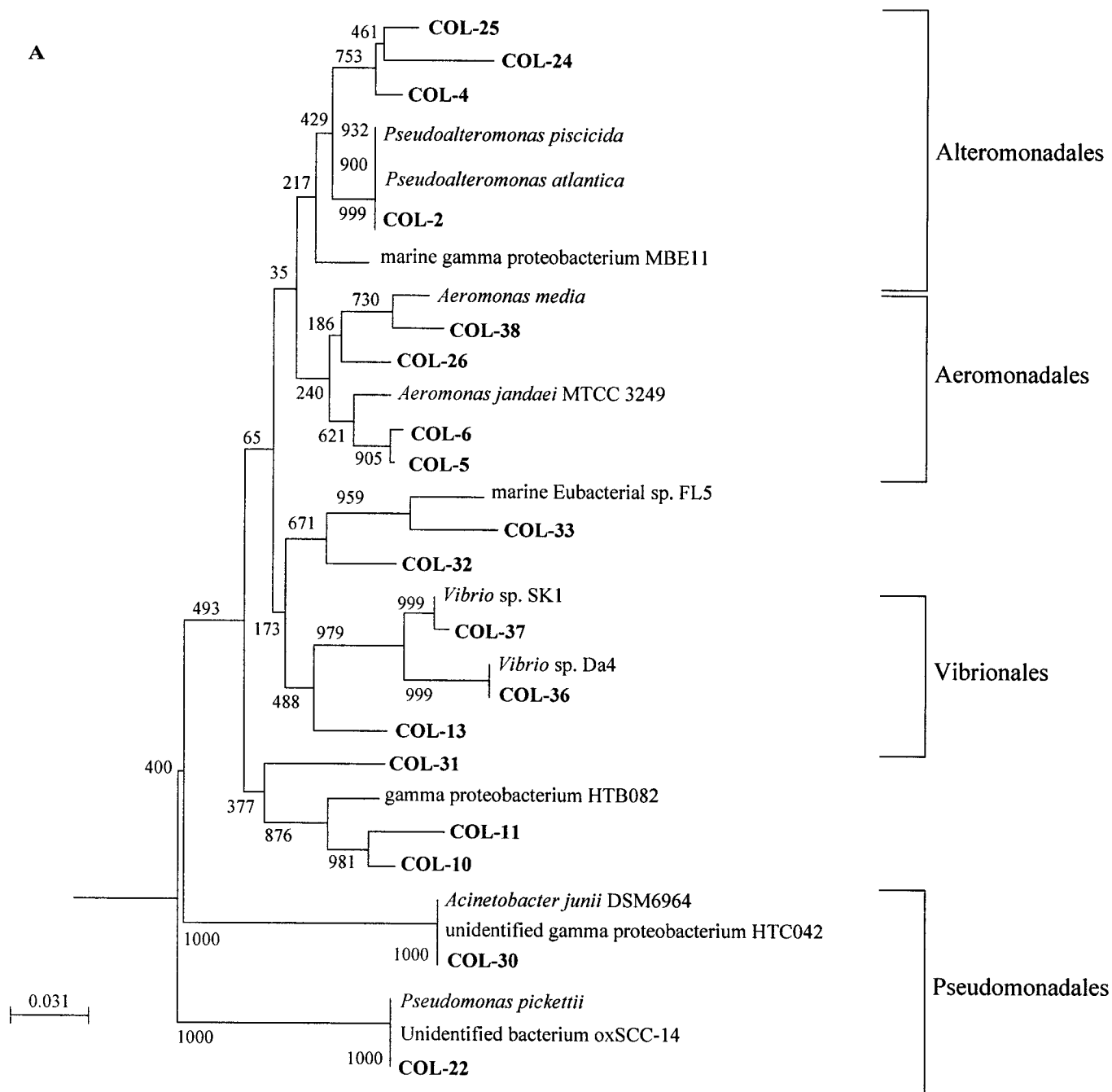


Fig. 4. Phylogenetic tree illustrating the relationships of sequenced bands (bold type) to major classes of bacteria. (A) Phylotypes grouping with the gamma class of proteobacteria (orders within the class are designated); (B) Phylotypes grouping with other classes of bacteria (a gamma proteobacteria is included for reference). The tree was inferred by neighbor joining method (Clustal W; Thompson et al. 1994) using the entire length of sequenced bands (~194 bp) beginning at the equivalent base to 341 and going toward the 3' end of the 16S rRNA molecule (*Escherichia coli* numbering). An archaeon, *Pyrococcus abyssi* ST549, was used as an outgroup. The number of bootstrap replicates supporting the branching order is shown above relevant nodes (out of 1,000 replicate samples). Scale bar indicates base pair substitutions per nucleotide position.

were also detected in these microcosms (Fig. 3A; FL-15, FL-18, COL-23) but they were a minor proportion of the phylotypes detected. Only one representative (COL-23, *Bradyrhizobium* sp. ORS285) was found among the colonizer population. This phylotype colonized detritus at 1 d but disappeared at 2 d. The other phylotypes from these two groups

were only detected in the  $<0.7 \mu\text{m}$  inoculum community prior to inoculation with diatom detritus.

Phylotypes most closely related to plastid DNA from cultured diatoms as well as from environmental plankton samples were detected at 1 d (PL-1 and PL-2; Fig. 4B; Table 2). Bands excised from incubations with the same diatom

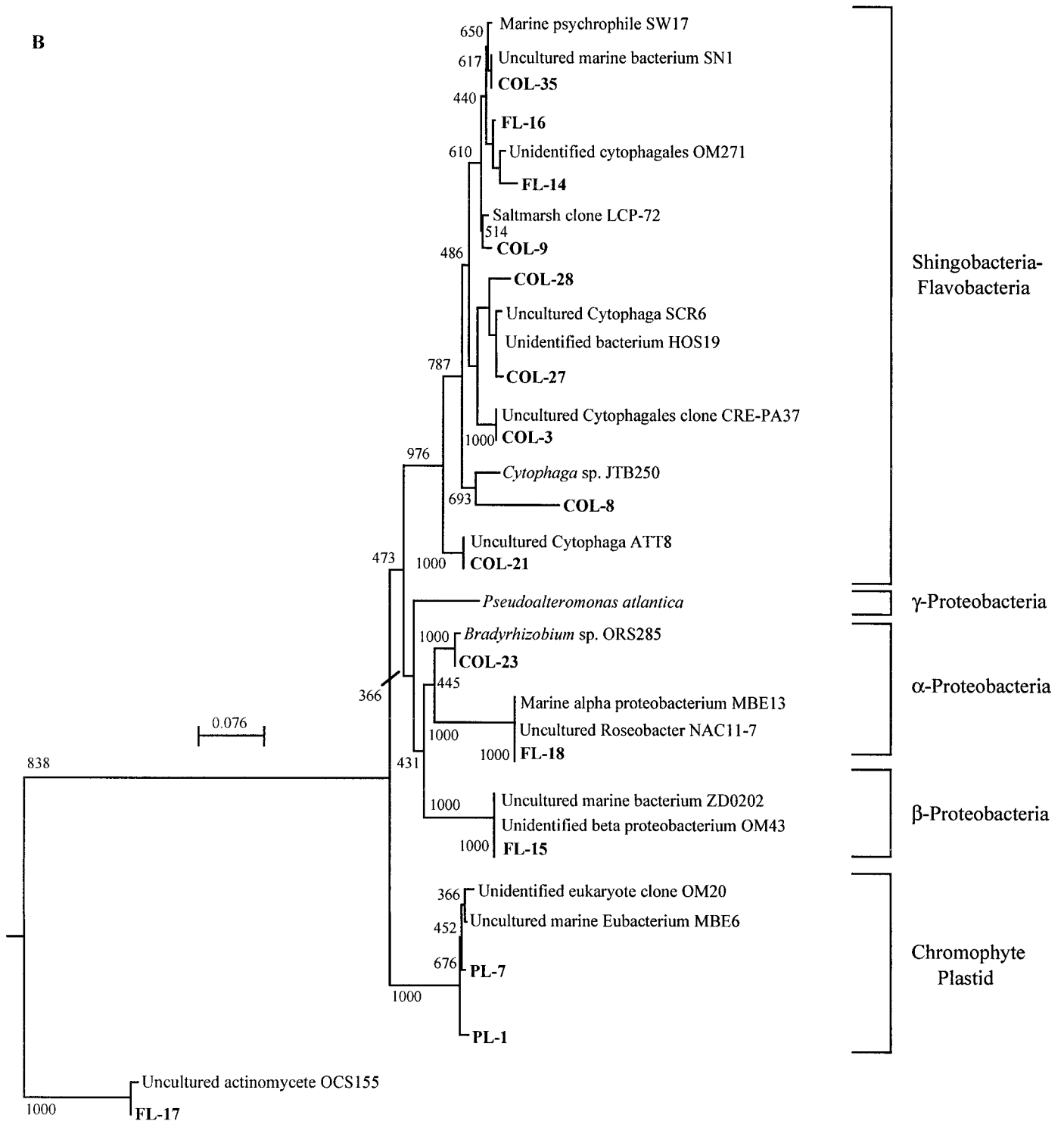


Fig. 4. Continued.

had identical sequences (bands 1 and 19 for *T. weissflogii*; bands 7 and 29 for *C. simplex*). Control experiments using DNA extracted from axenic *T. weissflogii* and *C. simplex* detritus verified that these bands were from the respective diatoms. These phlotypes were reduced dramatically by 2 d and remained at reduced band intensity throughout the

course of the sampling period (7 d), consistent with the degradation of diatoms by bacteria.

*Characterization of bacterial isolates*—Ectohydrolytic enzyme profiles (protease, glucosidase, lipase, and chitinase) and phylogenetic relationships were determined for 12 ma-

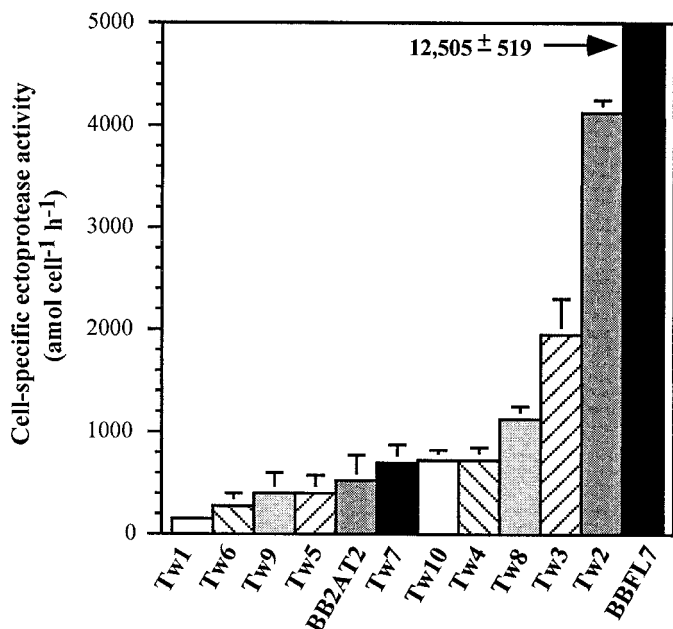


Fig. 5. Cell-specific protease activities of twelve marine isolates grown in ZoBell 2216E medium. Activities are expressed as hydrolysis rates of Leucine-AMC.

rine bacteria isolated from diatom enrichments and bottle bloom experiments. The cell-specific ectohydrolytic enzyme profile of each isolate was determined in order to examine the hydrolytic potential of each organism. Cell-specific protease activities varied by nearly three orders of magnitude (150 to 12,500 amol cell<sup>-1</sup> h<sup>-1</sup>; Fig. 5), which suggests very diverse proteolytic capabilities. BBFL7 had the highest cell-specific protease activity at 12,500 amol cell<sup>-1</sup> h<sup>-1</sup> followed by Tw2 and Tw3, which had activities of 4,100 and 1,900 amol cell<sup>-1</sup> h<sup>-1</sup>, respectively. Cell-specific activities of other ectohydrolyses displayed much narrower ranges. Lipase activities were at or below 250 for most isolates, although Tw1 and BB2AT2 showed enhanced activity (1,400 and 1,800 amol cell<sup>-1</sup> h<sup>-1</sup>, respectively). Glucosidase and chitinase activities were consistently the lowest activities measured with rates ranging from 0 to 50 amol cell<sup>-1</sup> h<sup>-1</sup> and from 0 to 70 amol cell<sup>-1</sup> h<sup>-1</sup>, respectively.

Nearly full-length (~1,500 bp) 16S rDNA gene sequences were obtained for all bacterial isolates examined. Phylogenetic analysis of gene sequences revealed that most of the isolates (Tw1 to Tw10, BB2AT2; 11 of 12) belonged to the  $\gamma$ -proteobacteria, whereas BBFL7 belonged to the SFB group (Fig. 6). Within the  $\gamma$ -proteobacteria, eight, one, and two isolates grouped with the *Alteromonadaceae*, *Vibrionaceae*, or *Oceanospirillaceae* families, respectively. All  $\gamma$ -proteobacteria sequences had >95% identity to their closest cultured relatives in the database except for Tw1, Tw2, and Tw3, which were only 94%, 93%, and 92% identical, respectively. The 16S rDNA gene sequence of BBFL7 also displayed low identity to its closest cultured relatives (92% and 89%, respectively, to 16S rRNA genes of *Cytophaga marinoflava* and *Flavobacterium* sp. 5N-3).

*Regeneration of diatom silica by bacterial isolates*—Each isolate was able to regenerate Si from *T. weissflogii* detritus during 10 d of exposure, although to varying degrees (Fig. 7). The final extent of Si regeneration among isolates varied by >300%, and  $V_{dis}$  ranged from 0.020 to 0.084. BBFL7 was most effective at causing particulate silica dissolution with >50% of particulate silica being regenerated in 10 d. Longer incubation (21 d) with BBFL7 resulted in nearly complete dissolution (90%) of particulate silica (data not shown). Other particularly effective isolates were Tw6, Tw7, and Tw8; Tw7 was most effective at causing silica dissolution during initial time periods (1–4 d). The least effective isolates were Tw4 and Tw5, resulting in 18% particulate Si dissolution in 10 d.

*Relationship between silica dissolution and ectoenzyme profile of bacterial isolates*—Of the ectohydrolytic enzyme activities determined for isolates grown in ZoBell 2216E medium, protease was most strongly correlated with Si regeneration. There was a strong linear relationship ( $r^2 = 0.55$ ) between silicon regeneration from *T. weissflogii* detritus after 10–16 d and the calculated protease activity exhibited on individual detritus cells. All other enzyme activities had much weaker correlation with Si regeneration. Linear regression  $r^2$  values for  $\alpha$ -glucosidase,  $\beta$ -glucosidase, lipase, and chitinase were 0.14, 0.26, 0.08, and 0.29, respectively.

The correlation between protease and Si regeneration was even stronger when protease activities were directly measured during exposure of each isolate to *T. weissflogii* detritus. Si regeneration after 10–16 d showed strong linear relationships with average cell-specific protease activities of bacterial colonizers ( $r^2 = 0.73$ ) and average protease activity encountered by *T. weissflogii* detrital cells ( $r^2 = 0.80$ ) (Fig. 8, closed symbols). These relationships were observed for nearly all experiments (18 of 19) using either bacterial isolates or natural bacterial assemblages (both types are included in Fig. 8). Interestingly, one experiment using isolate Tw3 did not follow this relationship (Fig. 8, open symbol). Epifluorescence microscopy revealed exceptionally intense colonization on *T. weissflogii* detritus (>200 bacteria diatom<sup>-1</sup>) by Tw3 along with aggregation of diatom detritus cells and film formation on aggregates.

## Discussion

The goal of this study was to reveal mechanistic controls on bacteria-mediated Si regeneration from diatom detritus. We examined the response of both natural bacterial assemblages and bacterial isolates to diatom detritus of known species identity and history. We emphasized the identity and ectoenzymatic activity of colonizing bacteria due to the importance of colonization to the process (Bidle and Azam 1999). Natural bacterial assemblages allowed us to test the consistency of Si regeneration by natural populations and to determine whether specific enzyme profiles and community composition were required for enhanced Si regeneration. The use of bacteria with known phylogenetic affiliations and ectoenzymatic profiles allowed detailed insight into the importance of species identity and ectohydrolytic activity. In all cases, the presence of bacteria stimulated silica dissolu-

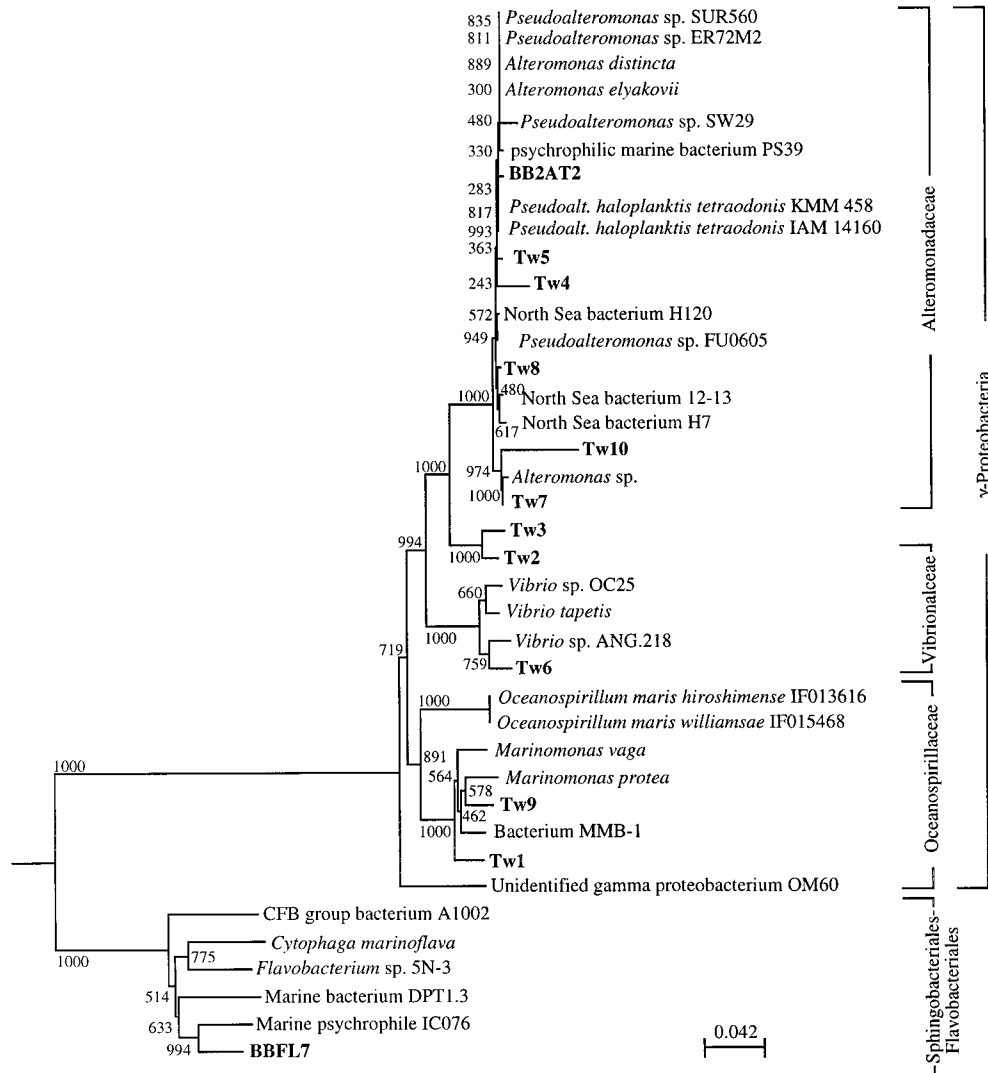


Fig. 6. Phylogenetic tree showing relationships of the 16S rDNA sequences for twelve marine isolates (bold type) to 16S rDNA genes of bacteria in different bacterial families. The tree was inferred by neighbor joining method using nearly full-length sequences in every case (~ 1500 bp). An archaeon (*Pyrococcus abyssi* ST549) was used as an outgroup. The number of bootstrap replicates supporting the branching order is shown above relevant nodes (out of 1,000 replicate samples). The scale bar indicates base pair substitutions per nucleotide position.

tion of diatom frustules over abiotic controls, consistent with previous findings (Patrick and Holding 1985; Bidle and Azam 1999). Bacteria-mediated Si regeneration was efficient, as regeneration rates were comparable to those of acid-digested detritus incubating under abiotic conditions. Since acid-digestion hydrolytically removes the organic matrix, it should represent the upper limit of Si regeneration from these diatoms. As reported in Bidle and Azam (1999), there was often considerable variability in the enhancement of particulate silica dissolution by natural bacterial assemblages collected on different dates. This variability (or lack thereof) allowed us to deduce controls on bacteria-mediated silicon regeneration.

*Proteolytic control of silicon regeneration*—Several lines of evidence support the conclusion that bacterial protease

was the principal ectohydrolytic activity controlling silica dissolution. First, experiments yielding extensive silica dissolution were consistently characterized by high cell-specific protease activities of colonizing bacteria. This was observed for both diatoms. It was especially pronounced for *T. weissflogii* detritus, where daily cell-specific protease activities during the first few days were elevated by at least an order of magnitude. For *C. simplex*, daily cell-specific protease activities during the first few days were at least two times higher in the experiment with more rapid silica dissolution. Statistically significant differences ( $p < 0.05$ ) in cell-specific protease activity were detected between experiments yielding fast and slow silica dissolution dynamics. Second, elimination of protease activity by the addition of protease inhibitors essentially halted particulate silica dissolution from both diatoms. The extent of silica dissolution after 10 d for

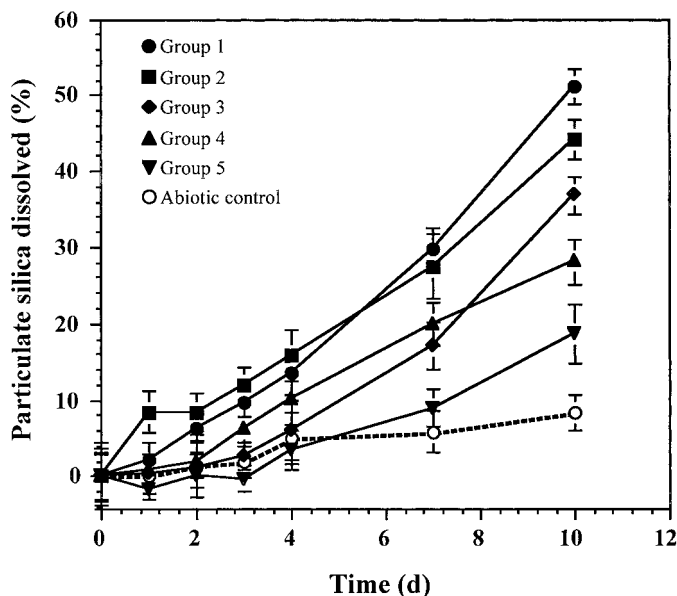


Fig. 7. Time course of particulate silica regeneration from *T. weissflogii* detritus incubated with twelve different marine isolates. Isolates that showed similar Si regeneration (within error bars of each other) were clustered into groups. Each group is represented by a different solid symbol (group 1 = BBFL7; group 2 = Tw7; group 3 = Tw6 and Tw8; group 4 = Tw1, Tw2, Tw3, Tw9, Tw10, BB2AT2; group 5 = Tw4 and Tw5). An abiotic control consisting of intact detritus resuspended in FASW is included for comparison (open symbols).

inhibited samples was an order of magnitude lower than that of uninhibited samples; in each case dissolution from inhibited samples resembled those of control incubations. Third, both cell-specific protease activities of bacterial colonizers and the protease activity exhibited on detritus were strongly correlated with silica dissolution from *T. weissflogii* detritus ( $r^2$  values were 0.74 and 0.80, respectively). These relationships held true for all but one of the experiments using either natural assemblages or bacterial isolates. No consistent relationship was found between glucosidase or lipase activities and enhanced silica dissolution, which suggests that general hydrolytic potential (Patrick and Holding 1985) does not control the process.

The control of Si regeneration by protease activity of colonizing bacteria is consistent with organized, protein-rich environments providing structural integrity to diatom frustules and protecting them against dissolution. New families of cell wall-associated proteins have been identified in diatoms (Kröger et al. 1994, 1996, 1997; Kröger and Sumper 1998) that have purported structural roles, and they are now well characterized. Frustulins are extractable with EDTA, and it is thought that they are associated via calcium bridges. Even though they were originally extracted from *Cylindrotheca fusiformis*, there is strong domain conservation within the frustulin family (Kröger et al. 1996). Antisera raised against an isoform of a 75 kilodalton frustulin ( $\alpha 1$  frustulin) from *C. fusiformis* recognized EDTA-extractable frustulins in cell walls from other diatoms (Kröger et al. 1994), which suggests that epitopes of frustulins are conserved among differ-

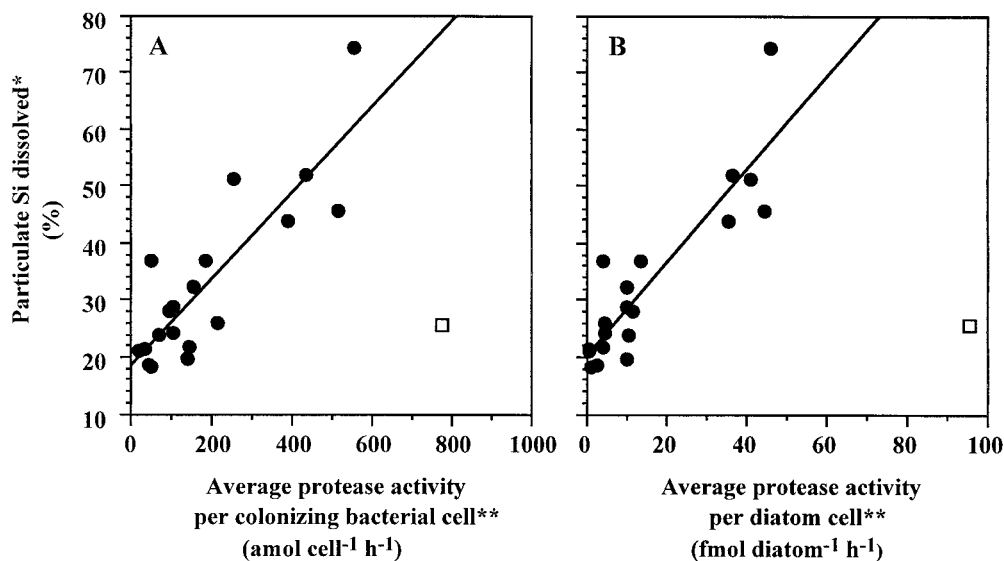


Fig. 8. Relationship between protease activity and the extent of particulate silica dissolution from *T. weissflogii* detritus. (A) cell-specific protease activity of colonizing bacterial cells and (B) protease activity exerted on individual detritus cells. Data from 19 separate incubations are pooled. Incubations used either a natural bacterial assemblage or a different bacterial isolate and is represented by a single point. Protease activities on diatom cells were calculated by multiplying cell-specific protease hydrolysis rates of colonizers by the average colonization intensity ( $n = 30$ ). Open symbols represent an experiment with Tw3 where intense aggregation and film formation was observed; solid symbols for all other experiments; \* after 10–16 d; \*\* using average hydrolysis rate of Leuine-AMC during 7 d of exposure. Regression lines are drawn through solid symbols (Panel A,  $y = 0.076x + 18.674$ ,  $r^2 = 0.74$ ; Panel B,  $y = 0.815x + 20.443$ ,  $r^2 = 0.80$ ).

ent species. Frustulins have been localized to the organic casing surrounding diatoms and were not associated with the silicalemma of newly formed silica deposition vesicles (Poll et al. 1999). Thus, frustulins do not appear to be directly involved in the polymerization of silica but provide a structural role in the organic casing. Other groups of proteins are directly associated with the silica-based substrate of the cell wall and are only extractable with hydrofluoric acid (hydrofluoric acid extractable proteins [HEPs] and silaffins). Rather than have a uniform distribution in *C. fusiformis* cell walls, HEPs colocalize with a distinct subset of silica girdle bands (Kröger et al. 1997). Silaffins directly promote polycondensation and precipitation of biogenic silica (Kröger et al. 1999) and they are thought to be directly involved in silica biomineralization. They are small (4–17 kD) polycationic peptides that contain features especially suited to promote silica flocculation at acidic pHs, the proposed environment of silica condensation within diatom cells.

Hydrolysis rate measurements in this study used amino acid and monosaccharide substrates, which were representative of molecules found to be enriched in diatom cell walls (Coombs and Volcani 1968; Hecky et al. 1973; Darley 1977). This should have provided bacterial ectoenzymes with substrates of similar composition to the diatom cell walls they were encountering. Protease activities were particularly elevated for glycine and serine substrates during the first few days, a result consistent with the fact that colonizing bacteria were experiencing proteins with enriched pools of these amino acids. Moreover, experiments with noticeably high activities using these substrates were characterized by enhanced silica dissolution, which indicates that these bacterial populations were able to efficiently hydrolyze the organic matrix. Protease activities measured with the leucine substrate were consistently high throughout the experiment even though leucine is not enriched in diatom cell walls. Elevated hydrolysis rates of Leucine-AMC may instead represent a general proteolytic response to generic protein pools.

The lack of a consistent relationship between glucosidase activity and silica dissolution argues against this enzyme activity controlling the process. In fact, most of the substrates used to test glucosidase activity yielded very low hydrolysis rates even for substrates that are enriched in cell wall polysaccharides (i.e., xylose and mannose). The biochemical compositions (percentage dry weight) of diatoms grown under nutrient replete conditions (like the ones used in this study) are characterized by a consistently higher contribution of protein compared to carbohydrates (Parsons et al. 1961; Werner 1966). This has also been seen for a coastal phytoplankton community, which was dominated by diatoms (Werner 1966). Even though it was not examined in this study, it would be interesting to determine the relative contributions of protease and glucosidase in response to diatoms that had been grown in nitrogen-limiting conditions. Such conditions result in total cellular pools that are more enriched in carbohydrates for both cultured and coastal phytoplankton communities (Werner 1966) and may result in an increased role for glucosidase activity in Si regeneration.

*Importance of colonizer identity*—The fact that bacterial source populations collected for experiments 2 and 3 did not behave similarly with the two different diatoms revealed that community composition significantly controlled Si regeneration. Diatom species identity played a significant role by influencing the diversity of colonizing bacteria as well as the susceptibility of detritus to hydrolytic action. In these experiments, similar Si regeneration was caused by bacterial assemblages exposed to *T. weissflogii*, which provided insight into “consistency controls.” Both the ectoprotease profiles and community compositions of colonizing bacteria in these experiments were remarkably similar. Very high cell-specific protease activities of the colonizing bacteria were observed for experiments 2 and 3. No statistically significant differences were detected between average cell-specific protease activity during the experiments, which indicates that detritus encountered similar hydrolytic pressures. Furthermore, similar phylotypes from  $\gamma$ -proteobacteria and SFB groups consistently colonized *T. weissflogii* detritus during these experiments, especially those most closely related to *P. atlantica*, *Pseudoalteromonas* sp. A3, and several uncultured Cytophaga.

Unlike *T. weissflogii*, *C. simplex* had very different dissolution profiles for experiments 2 and 3, with the latter resulting in twice as much particulate silica dissolution. Comparisons of community compositions and cell-specific protease activities provided insight into “variability controls” of Si regeneration. The cell-specific protease activities of colonizing bacteria were at least twice as high for experiment 3 as experiment 2, especially in the first few days. There were particularly noticeable differences in the levels of cell-specific protease activity at 0–1 d, especially for glycine and serine substrates. Furthermore, distinct differences in colonizer community composition were consistent with differences observed in ectoprotease activities. Experiment 2 displayed little to no initial diversity on detritus since the only phylotype detected at 1 d was that of *C. simplex* plastid DNA. In contrast, experiment 3 had a much higher initial diversity. Phylotypes corresponding to *P. atlantica*, an uncultured Cytophaga, two unclassified *Pseudomonas* sp., *Bradyrhizobium elkanii*, and an unidentified  $\gamma$ -proteobacteria were detected at 1 d. Most of these phylotypes had been replaced within 2 d, which suggests rapid turnover of much of the initial colonizing community. Even though most of the phylotypes developing on *C. simplex* detritus after 2 d were  $\gamma$ -proteobacteria, their identity in experiment 3 was different than those detected in experiment 2. For example, experiment 2 was characterized by *Collwellia demingiae*, an unknown  $\gamma$ -proteobacterium, and *P. atlantica* phylotypes, while experiment 3 was characterized by *P. atlantica*, two unique unidentified  $\gamma$ -proteobacteria, *Alteromonas* sp., *Aeromonas* sp., *Ferrimonas balearica*, and *Vibrio* species. These results suggest that time of colonization and diversity of colonizing phylotypes were critical factors responsible for rapid Si regeneration from *C. simplex*. These results also suggest that *Alteromonas* sp., *Aeromonas* sp., and *Vibrio* sp. possess particularly effective colonization and ectohydrolytic capabilities that lead to enhanced Si regeneration. This point is supported by the observation that two of the most effective bacterial isolates in regenerating diatom silicon from *T.*

*weissflogii* were most closely related to *Vibrio* sp. (Tw6) and *Alteromonas* sp. (Tw7).

The predominance of particular phylotypes on diatom detritus was interpreted as an indication of their marked role in colonizing and degrading diatom organic matter (eventually leading to silica dissolution). Even though DGGE analysis of PCR amplicons possesses potential biases, we assume that it reflects the major variations in the relative abundance of PCR-amplifiable phylotypes. Replicate PCR and DGGE gels confirmed that profiles are highly reproducible, which led us to assume there is a comparable amplification bias for or against a certain sequence. We thus assumed that changes in the relative band intensity with time reflect actual changes in the relative abundance of a phylotype. However, we caution that DGGE does not provide a complete or quantitative view of bacterial community composition, but rather a more simplified "fingerprint." An interesting observation during this study was that colonization was often quite dynamic, with some phylotypes appearing rapidly and displaying highly variable residence times on diatom detritus. For example, COL-2 colonized very early and persisted throughout each experiment, which suggests that this phylotype possessed strong ability to respond to diatoms. Many phylotypes displayed very rapid and significant bursts of growth on diatom detritus as indicated by banding patterns. Several phylotypes that were undetected in inoculum community were observed as strong colonizers of diatom detritus after one day of exposure. Also, many colonizing phylotypes were detected at 2 d following a noticeable absence at 1 d. In some cases these rapid bursts of growth were followed by very rapid turnover, where dominant phylotypes disappeared and were replaced by unique phylotypes. This was especially evident in experiment 3, where the community composition of colonizing bacteria was very dynamic. Viral attack (Fuhrman 1999) and allelopathy (Long et al; Long and Azam, pers. comm.) against particular bacterial colonizers might explain the rapid turnover of distinct bacterial phylotypes. These processes could heavily influence whether bacterial phylotypes that are effective at causing enhanced silicon regeneration develop on diatom detritus.

Representatives from the domain Archaea were not detected among colonizing populations, which argues against their role in promoting Si regeneration. Archaeal phylotypes have been detected in various marine environments (DeLong 1992; Fuhrman et al. 1993; DeLong 1998) and have recently been shown to dominate mesopelagic zones (Karner et al. 2001), but they have not been found to be associated with diatoms (which argues against transport via sinking phyto-detrital aggregates). Instead, bacterial phylotypes from  $\gamma$ -proteobacteria and SFB groups dominated colonizing populations in this study, which suggests they play important roles in transforming organic and inorganic matter from diatoms. Representatives from these groups have been found among marine bacterioplankton communities from various environments, including the Antarctic (Bowman et al. 1997), the North Carolina continental shelf (Rappé et al. 1997), and coastal California waters (Cottrell and Kirchman 2000a). Phylotypes in this study were closely related to those observed on marine macroaggregates (DeLong et al. 1993),

during a mesocosm diatom bloom (Riemann et al. 2000), in Antarctic ice diatom assemblages (Bowman et al. 1997), during a dinoflagellate bloom (Fandino et al. 2001), in coastal picoplankton (Rappé et al. 1997), and on particles off the coast of Oregon (Crump et al. 1999). This is an interesting result since our study used very defined experimental systems composed of axenic diatom detritus. Riemann et al. (2000) also found that  $\alpha$ -proteobacteria dominated colonizing phylotypes during a diatom bloom consisting primarily of *Thalassiosira* species. Our study did not detect  $\alpha$ -proteobacteria as major colonizers, but other studies have also found  $\alpha$ -proteobacteria associated with marine phytoplankton (Crump et al. 1999; González et al. 2000).

*Si regeneration by bacterial isolates*—The isolates used in this study represented the major groups of bacteria that colonized detritus from natural assemblages. They also provided a broad range of hydrolytic potential. Therefore, studies using these bacterial isolates provided detailed insight into the effectiveness of  $\gamma$ -proteobacteria and SFB groups at colonizing and degrading diatom detritus. All isolates demonstrated an ability to cause particulate silica dissolution from *T. weissflogii* detritus, but the extent of dissolution varied by >300% after 10 d. Regardless of phylogenetic affiliation, isolates with enhanced cell-specific protease activity and colonization abilities were most effective at regenerating Si. BBFL7, a representative of the SFB group, was the most effective isolate tested. BBFL7 possessed very high cell-specific protease activities and colonization ability, a trait common to many SFB representatives. Recently, this bacteria cluster has been shown to be a major component of natural assemblages consuming protein (Cottrell and Kirchman 2000b), which suggests this group is particularly effective at using proteinaceous substrates. A few representatives from the  $\gamma$ -proteobacteria (Tw6, Tw7, and Tw8) were also particularly effective at causing extensive silica dissolution; they were most closely related to *Vibrio* sp., *Alteromonas* sp., and *Pseudoalteromonas* sp., respectively. Our results are consistent with those of Patrick and Holding (1985), who also found that isolates representing  $\gamma$ -proteobacteria and Flavobacteria were effective at causing silica dissolution from diatoms.

Interestingly, Si regeneration varied considerably (>200%) among eight closely related *Alteromonadaceae*, which suggests that the potential of closely related bacteria to colonize and degrade diatom detritus cannot be deduced on group affiliations alone. Our results suggest that very closely related species may occupy different microniches, with some representatives being particularly suited to diatoms. Recently, it was shown that bacterial species richness increases at millimeter scales in response to organic matter loads such as a phytoplankton bloom (Long and Azam, pers. comm.). Presumably, this increase in bacterial species richness and diversity is in response to an increased diversity of microniches within the organic matter field, which allows more bacterial phylotypes to coexist. Our results have implications for the interpretation of community hybridization studies using probes for bacterial divisions and subclasses typically comprising marine assemblages (Glöckner et al. 1999; Cottrell and Kirchman 2000b). In recent years, there

has been considerable interest in determining the relative contribution of various phylogenetic groups to biochemically transform and use organic matter in the sea. Results can reveal strategies that a particular group uses in processing organic matter. However, the wide variability in response to diatom detritus observed in this study suggests that there is considerable variability in the strategies and capabilities of organic matter transformation within a family. More data are needed to determine whether the variability seen among the *Alteromonadaceae* also exists within other families, but it seems prudent to interpret hybridization data with caution.

In most instances, the presence of intense bacterial colonization and hydrolytic activity greatly enhanced the solubilization of particulate silica. However, some of our data suggest that bacterial activity can also inhibit the recycling of silicon into the bulk water. Isolate Tw3 consistently colonized *T. weissflogii* detritus and displayed the highest ectoprotease activities measured on detritus, but it caused only modest silicon regeneration. Visible diatom aggregation and the production of an exopolymeric film around aggregates characterized incubations containing Tw3. Tw3 most likely hydrolyzed the organic matrix surrounding *T. weissflogii* frustules and caused significant silica dissolution. Dissolved silicic acid may have been retained within the interstitial water of individual aggregates by the exopolymeric film. This phenomenon has been observed for natural marine snow where intensive silica cycling led to  $\text{Si}(\text{OH})_4$  concentrations as high as  $305 \mu\text{M}$  in interstitial fluids and where the Si diffusion coefficient was reduced by two orders of magnitude compared to that in pure seawater (Brzezinski et al. 1997a). Alternatively, it is possible that acid production during bacterial metabolism lowered the pH of interstitial water and bathed silica frustules in an environment less conducive for dissolution. Irrespective of the mechanism involved, these results suggest that bacteria can also greatly reduce the extent of Si regeneration within the upper water column by causing diatom detritus to aggregate (increasing sinking flux) and by forming exopolymers around aggregated cells (decreasing Si diffusion coefficients). Detailed study is needed to further examine the role of aggregation on silicon regeneration, but it should be considered as a control mechanism that is highly dependent on bacterial species composition.

*Implications for previous studies*—The goal of this study was to reveal detailed mechanistic insight into the factors that control bacteria-mediated Si regeneration from diatom detritus. It builds on previous work by providing both a mechanism for highly variable ( $<0.1$  to  $>1.0$ ) silica  $D:P$  ratios (Nelson et al. 1995) in various oceanic systems and an explanation for highly variable (about fourfold) silicon regeneration rates by natural bacterial assemblages (Bidle and Azam 1999). The control mechanisms observed in this study also provide detailed insight into previous experimental studies of biogenic silica dissolution performed under controlled laboratory conditions and at sea. Our measured  $V_{\text{dis}}$  values for detritus incubating with bacteria ( $0.016$ – $0.084 \text{ d}^{-1}$ ) are consistent with previous *in vitro* studies using untreated and acid-cleaned diatom material (Kamatani 1969; Kamatani and Riley 1979; Kamatani 1982; Hurd and Bird-

whistell 1983). These studies have shown that  $V_{\text{dis}}$  increases systematically with the specific surface area of diatom silica ( $A_{\text{sp}}$  in  $\text{m}^2 \text{ g}^{-1}$ ) and with temperature. Our results suggest that colonization intensity and bacterial protease activity control dissolution by denuding diatoms of their protective organic matrix and increasing the surface area of naked silica that is exposed to dissolution. Moreover, proteolytic activities and the resulting clearance rates of the organic matrix are strongly temperature dependent (Bidle and Azam, unpubl.). Increases in temperature will result in more efficient removal of organic carbon along with faster chemical dissolution rates. Our results also provide an explanation for the observed trends in  $V_{\text{dis}}$  in various field studies (Nelson and Goering 1977; Nelson and Gordon 1982; Brzezinski and Nelson 1989). Field measurements have shown that  $V_{\text{dis}}$  is often lowest in the upper few meters of the water column and increases significantly with depth down to 50–80 m. Since  $V_{\text{dis}}$  is normalized to diatom biomass ( $\text{BSiO}_2$ ), higher dissolution rates with depth are due to the presence of silica that dissolves more readily than at the surface rather than from an increase in particle density. The low  $V_{\text{dis}}$  values reported in this study for axenic diatom detritus incubating in the absence of bacterial degradation ( $0.004$ – $0.009 \text{ d}^{-1}$ ) are consistent with those measured in field studies near the surface, and they indicate that low surface  $V_{\text{dis}}$  is due to the preponderance of intact (mostly living) diatoms. Furthermore, the dependence of  $V_{\text{dis}}$  on colonization and protease activity in this study strongly suggests that the higher  $V_{\text{dis}}$  values measured with depth are due to a much higher fraction of detrital silica whose protective organic coating has been removed by bacterial proteases as it sinks through the water column.

Bacterial species identity strongly controlled silicon regeneration by influencing the colonization potential and ectohydrolytic profiles of bacteria as well as the formation of phytodetrital aggregates. The fact that bacteria can both enhance and deter silicon regeneration shows how variability in species composition and activity can significantly dictate the extent of silica cycling within the upper 200 m. Clearly, the composition of colonizing bacterial populations and their attendant enzyme activities will determine whether *in situ* silicon regeneration rates are fast or slow in nature. Regeneration rates will also be modulated by other ecosystem parameters, particularly those affecting bacterial activity on diatoms. Factors that affect the dynamics of dominant colonizing phylotypes, such as viral infection and bacteria-bacteria antagonistic interactions, may play important roles in determining whether effective populations develop on decaying diatoms. Mechanistic models of oceanic silica cycling should incorporate these variables for predictions of silicon regeneration.

## References

- ALTSCHUL, S. F., W. GISH, W. MILLER, E. W. MYERS, AND D. J. LIPMAN. 1990. Basic local alignment search tool. *J. Mol. Biol.* **215**: 403–410.
- BIDLE, K. D., AND F. AZAM. 1999. Accelerated dissolution of diatom silica by natural marine bacterial assemblages. *Nature* **397**: 508–512.

- BOWMAN, J. P., S. A. MCCAMMON, M. V. BROWN, D. S. NICHOLS, AND T. A. McMEEKIN. 1997. Diversity and association of psychrophilic bacteria in Antarctic sea ice. *Appl. Environ. Microbiol.* **63**: 3068–3078.
- BRZEZINSKI, M. A., A. L. ALLDREDGE, AND L. M. O'BRYAN. 1997a. Silica cycling within marine snow. *Limnol. Oceanogr.* **42**: 1706–1713.
- , AND D. M. NELSON. 1989. Seasonal changes in the silicon cycle within a Gulf Stream warm-core ring. *Deep-Sea Res.* **36**: 1009–1030.
- , AND ———. 1995. The annual silica cycle in the Sargasso Sea near Bermuda. *Deep-Sea Res.* **42**: 1215–1237.
- , AND ———. 1996. Chronic substrate limitation of silicic acid uptake rates in the western Sargasso Sea. *Deep-Sea Res.* **43**: 437–453.
- , D. R. PHILLIPS, F. P. CHAVEZ, G. E. FRIEDERICH, AND R. C. DUGDALE. 1997b. Silica production in the Monterey, California, upwelling system. *Limnol. Oceanogr.* **42**: 1694–1705.
- , T. A. VILLAREAL, AND F. LIPSCHULTZ. 1998. Silica production and the contribution of diatoms to new and primary production in the central North Pacific. *Mar. Ecol. Prog. Ser.* **167**: 89–104.
- COOMBS, J., AND B. E. VOLCANI. 1968. Studies on the biochemistry and fine structure of silica-shell formation in diatoms: Chemical changes in the wall of *Navicula pelliculosa* during its formation. *Planta* **82**: 280–292.
- COTTRELL, M. T., AND D. L. KIRCHMAN. 2000a. Community composition of marine bacterioplankton determined by 16S rRNA gene clone libraries and fluorescence in situ hybridization. *Appl. Environ. Microbiol.* **66**: 5116–5122.
- , AND ———. 2000b. Natural assemblages of marine proteobacteria and members of the Cytophaga-Flavobacter cluster consuming low- and high-molecular-weight dissolved organic matter. *Appl. Environ. Microbiol.* **66**: 1692–1697.
- CRUMP, B. C., E. V. ARMBRUST, AND J. A. BAROSS. 1999. Phylogenetic analysis of particle-attached and free-living bacterial communities in the Columbia River, its estuary, and the adjacent coastal ocean. *Appl. Environ. Microbiol.* **65**: 3192–3204.
- DARLEY, W. M. 1977. Biochemical composition, p. 198–223. *In* D. Werner [ed.], *The biology of diatom, botanical monographs*. Blackwell.
- DELONG, E. 1998. Archaeal means and extremes. *Science* **280**: 542–543.
- DELONG, E. F. 1992. Archaea in coastal marine environments. *Proc. Natl. Acad. Sci. USA* **89**: 5685–5689.
- , D. G. FRANKS, AND A. L. ALLDREDGE. 1993. Phylogenetic diversity of aggregate-attached vs. free-living marine bacterial assemblages. *Limnol. Oceanogr.* **38**: 924–934.
- DON, R. H., P. T. COX, B. J. WAINWRIGHT, K. BAKER, AND J. S. MATTICK. 1991. "Touchdown" PCR to circumvent spurious priming during gene amplification. *Nucleic Acids Res.* **19**: 4008.
- DUGDALE, R. C., AND F. P. WILKERSON. 1998. Silicate regulation of new production in the equatorial Pacific upwelling. *Nature* **391**: 270–273.
- , AND H. J. MINAS. 1995. The role of a silicate pump in driving new production. *Deep-Sea Res.* **42**: 697–719.
- FANDINO, L. B., L. RIEMANN, G. F. STEWARD, R. A. LONG, AND F. AZAM. 2001. Variations in bacterial community structure during a dinoflagellate bloom analyzed by DGGE and 16S rDNA sequencing. *Aquat. Microb. Ecol.* **23**: 119–130.
- FUHRMAN, J. A. 1999. Marine viruses and their biogeochemical and ecological effects. *Nature* **399**: 541–548.
- , D. E. COMEAU, Å. HAGSTROM, AND A. M. CHAN. 1988. Extraction from natural planktonic microorganisms of DNA suitable for molecular biological studies. *Appl. Environ. Microbiol.* **54**: 1426–1429.
- , K. MCCALLUM, AND A. A. DAVIS. 1993. Phylogenetic diversity of subsurface marine microbial communities from the Atlantic and Pacific Oceans. *Appl. Environ. Microbiol.* **59**: 1294–1302.
- GLÖCKNER, F. O., B. M. FUCHS, AND R. AMANN. 1999. Bacterioplankton compositions of lakes and oceans: A first comparison based on fluorescence in situ hybridization. *Appl. Environ. Microbiol.* **65**: 3721–3726.
- GONZÁLEZ, J. M., R. SIMÓ, R. MASSANA, J. S. COVERT, E. O. CASAMAYOR, C. PEDRÓS-ALIÓ, AND M. A. MORAN. 2000. Bacterial community structure associated with a dimethylsulfoniopropionate-producing north Atlantic algal bloom. *Appl. Environ. Microbiol.* **66**: 4237–4246.
- GUILLARD, R. R. L. 1975. Culture of phytoplankton for feeding marine invertebrates, p. 26–60. *In* W. L. Smith and M. H. Chanley [eds.], *Culture of marine invertebrate animals*. Plenum.
- HECKY, R. E., K. MOPPER, P. KILHAM, AND E. T. DEGENS. 1973. The amino acid and sugar composition of diatom cell-walls. *Mar. Biol.* **19**: 323–331.
- HONJO, S., J. DYMOND, R. COLLIER, AND S. J. MANGANINI. 1995. Export production of particles to the interior of the equatorial Pacific Ocean during the 1992 EqPac experiment. *Deep-Sea Res.* **42**: 831–870.
- HOPPE, H. G. 1983. Significance of exoenzymatic activities in the ecology of brackish water: Measurements by means of methylumbelliferyl-substrates. *Mar. Ecol. Prog. Ser.* **11**: 299–308.
- HURD, D. C., AND S. BIRDWHISTELL. 1983. On producing a general model for biogenic silica dissolution. *Am. J. Sci.* **283**: 1–28.
- KAMATANI, A. 1969. Regeneration of inorganic nutrients from diatom decomposition. *J. Oceanogr. Soc. Jpn.* **25**: 63–74.
- . 1982. Dissolution rates of silica from diatoms decomposing at various temperatures. *Mar. Biol.* **68**: 91–98.
- , AND J. P. RILEY. 1979. Rate of dissolution of diatom silica walls in seawater. *Mar. Biol.* **55**: 29–35.
- KARNER, M. B., E. F. DELONG, AND D. M. KARL. 2001. Archaeal dominance in the mesopelagic zone of the Pacific Ocean. *Nature* **409**: 507–510.
- KRÖGER, N., C. BERGSDORF, AND M. SUMPER. 1994. A new calcium binding glycoprotein family constitutes a major diatom cell wall component. *EMBO J.* **13**: 4676–4683.
- , ———, AND ———. 1996. Frustulins: Domain conservation in a protein family associated with diatom cell walls. *Eur. J. Biochem.* **239**: 259–264.
- , R. DEUTZMANN, AND M. SUMPER. 1999. Polycationic peptides from diatom biosilica that direct silica nanosphere formation. *Science* **286**: 1129–1132.
- , G. LEHMANN, R. RACHEL, AND M. SUMPER. 1997. Characterization of a 200-kDa diatom protein that is specifically associated with a silica-based substructure of the cell wall. *Eur. J. Biochem.* **250**: 99–105.
- , AND M. SUMPER. 1998. Diatom cell wall proteins and the cell biology of silica biomineralization. *Protist* **149**: 213–219.
- LEWIN, J. C. 1961. The dissolution of silica from diatom walls. *Geochim. Geophys. Acta* **21**: 182–198.
- . 1962. Silicification, p. 445–455. *In* R. E. Lewin [ed.], *Physiology and biochemistry of algae*. Academic.
- MUYZER, G., E. C. D. WAAL, AND A. G. UITTERLINDEN. 1993. Profiling of complex microbial populations by denaturing gradient gel electrophoresis analysis of polymerase chain reaction-amplified genes coding for 16S rRNA. *Appl. Environ. Microbiol.* **59**: 695–700.
- NELSON, D. M., AND M. A. BRZEZINSKI. 1990. Kinetics of silicic

- acid uptake by natural diatom assemblages in two Gulf Stream warm-core rings. *Mar. Ecol. Prog. Ser.* **62**: 283–292.
- , D. J. DEMASTER, R. B. DUNBAR, AND J. W. O. SMITH. 1996. Cycling of organic carbon and biogenic silica in the Southern Ocean: Estimates of water-column and sedimentary fluxes on the Ross Sea continental shelf. *J. Geophys. Res.* **101**: 18,519–18,532.
- , AND Q. DORTCH. 1996. Silicic acid depletion and silicon limitation in the plume of Mississippi River: Evidence from kinetic studies in spring and summer. *Mar. Ecol. Prog. Ser.* **136**: 163–178.
- , AND J. J. GOERING. 1977. Near-surface silica dissolution in the upwelling region off northwest Africa. *Deep-Sea Res.* **24**: 65–73.
- , AND L. I. GORDON. 1982. Production and pelagic dissolution of biogenic silica in the Southern Ocean. *Geochim. Cosmochim. Acta* **46**: 491–501.
- , AND P. TRÉGUER. 1992. Role of silicon as a limiting nutrient to Antarctic diatoms: Evidence from kinetic studies in the Ross Sea ice-edge zone. *Mar. Ecol. Prog. Ser.* **80**: 255–264.
- , ———, M. A. BRZEZINSKI, A. LEYNAERT, AND B. QUÉGUINER. 1995. Production and dissolution of biogenic silica in the ocean: Revised global estimates, comparison with regional data and relationship to biogenic sedimentation. *Glob. Biogeochem. Cycles* **9**: 359–372.
- PARSONS, T. R., Y. MAITA, AND C. M. LALLI. 1984. A manual of chemical and biological methods for seawater analysis. Pergamon.
- , K. STEPHENS, AND J. D. H. STRICKLAND. 1961. On the chemical composition of eleven species of marine phytoplankters. *J. Fish. Res. Board Can.* **18**: 1001–1016.
- PATRICK, S., AND A. J. HOLDING. 1985. The effect of bacteria on the solubilization of silica in diatom frustules. *J. Appl. Bacteriol.* **59**: 7–16.
- POLL, W.H.V.D., E. G. VRIELING, AND W. W. C. GIESKES. 1999. Location and expression of frustulins in the pennate diatoms *Cylindrotheca fusiformis*, *Navicula pelliculosa*, and *Navicula salinarium* (Bacillariophyceae). *J. Phycol.* **35**: 1044–1053.
- RAPPÉ, M. S., P. F. KEMP, AND S. J. GIOVANNONI. 1997. Phylogenetic diversity of marine coastal picoplankton 16S rRNA genes cloned from the continental shelf off Cape Hatteras, North Carolina. *Limnol. Oceanogr.* **42**: 811–826.
- RIEMANN, L., G. F. STEWARD, AND F. AZAM. 2000. Dynamics of bacterial community composition and activity during a mesocosm diatom bloom. *Appl. Environ. Microbiol.* **66**: 578–587.
- , ———, L. B. FANDINO, L. CAMPBELL, M. R. LANDRY, AND F. AZAM. 1999. Bacterial community composition during two consecutive NE Monsoon periods in the Arabian Sea studied by denaturing gradient gel electrophoresis (DGGE) of rRNA genes. *Deep-Sea Res. II* **46**: 1791–1811.
- SAMBROOK, J., E. F. FRITSCH, AND T. MANIATIS. 1989. Molecular cloning: A laboratory manual. Cold Spring Harbor Laboratory Press.
- SHEFFIELD, V. C., D. R. COX, L. S. LERMAN, AND R. M. MYERS. 1989. Attachment of a 40-base-pair G+C-rich sequence (GC-clamp) to genomic DNA fragments by the polymerase chain reaction results in improved detection of single-base changes. *Proc. Natl. Acad. Sci. USA* **86**: 232–236.
- SIERACKI, M. E., P. G. VERITY, AND D. K. STOECKER. 1993. Plankton community response to sequential silicate and nitrate depletion during the 1989 North Atlantic spring bloom. *Deep-Sea Res. II* **40**: 213–225.
- SMITH, C. R., D. J. HOOVER, S. E. DOAN, R. H. POPE, D. J. DEMASTER, F. C. DOOBS, AND M. A. ALTABET. 1996. Phytodetritus at the abyssal seafloor across 10° of latitude in the central equatorial Pacific. *Deep-Sea Res. II* **43**: 1309–1338.
- TANDE, K. S., AND D. SLAGSTAD. 1985. Assimilation efficiency in herbivorous aquatic organisms—the potential of the ratio method using <sup>14</sup>C and biogenic silica as markers. *Limnol. Oceanogr.* **30**: 1093–1099.
- THOMPSON, J. D., D. E. HIGGINS, AND T. J. GIBSON. 1994. Clustal W: Improving the sensitivity of progressive multiple sequence alignment through sequence weighting, position-specific gap penalties and weight matrix choice. *Nucleic Acids Res.* **22**: 4673–4680.
- TRÉGUER, P., D. M. NELSON, A. J. V. BENNEKOM, D. J. DEMASTER, A. LEYNAERT, AND B. QUÉGUINER. 1995. The silica balance in the world ocean: A reestimate. *Science* **268**: 375–379.
- WERNER, D. 1966. Die Kieselsäure im Stoffwechsel von *Cyclotella cryptica* Reimann, Lewin und Guillard. *Arch. Microbiol.* **55**: 278–308.

Received: 16 March 2001

Accepted: 9 July 2001

Amended: 12 July 2001